Polyoxometalate-based Photoactive Hybrid: uncover the first crystal structure of covalently linked hexavanadate-porphyrin molecule

Yingting Zhu,[†] Yichao Huang,[†]* Qi Li,[†] Dejin Zang,[†] Jing Gu,[‡]* Yajie Tang,[§] and Yongge Wei[†]*

[†] Key Lab of Organic Optoelectronics & Molecular Engineering of Ministry of Education, Department of Chemistry, Tsinghua University, Beijing 100084, China.

[‡] Department of Chemistry and Biochemistry, San Diego State University, 5500 Campanile Drive, San Diego, CA 92182-1030, USA

[§] Key Laboratory of Fermentation Engineering (Ministry of Education), Hubei Provincial Cooperative Innovation Center of Industrial Fermentation, Hubei Key Laboratory of Industrial Microbiology, Hubei University of Technology, Wuhan 430068, P. R. China.

*Corresponding Author:

E-mail: yichaoh@126.com (Y.C.H.)

E-mail: yonggewei@mail.tsinghua.edu.cn (Y.G.W.)

E-mail: jgu@sdsu.edu (J.G.)

Contents

Reagents and Instruments 3
Table S1 4
Table S2 5
1. Synthesis of Porphyrin Organic Building Blocks 6
2. ^{1}H-NMR 8
3. ESI-MS analysis 10
4. FT-IR 11
5. UV-Vis absorption and emission spectra 13
6. Photocatalytic activities 14
7. FT-IR spectra before and after photocatalysis 18
8. Energy bandgap calculation and CV results 19
Table S3 20
References 21

Reagents and Instruments

All reagents were purchased without further treatment except dimethylacetamide (DMAC). DMAC was dried with calcium hydride before use. ^{1}H-NMR spectra were recorded using a JEOL JNM-EXC 400 spectrometer. ESI-MS spectra were recorded on a Thermo Q Exactive spectrometer. UV-Vis spectra were recorded on a UNICO UV-2102PC spectrophotometer in the range 300-800 nm. Elemental analysis was measured with Elementar Vario EL III element analyzer. Infrared spectroscopy was recorded on a Bruker Vertex FT-IR spectrometer with a diamond ATR mode in the range of 600−4000 cm^{-1}. V6 represents $(Bu_4N)_2[V_6O_{13}\{(OCH_2)_3CCH_2OH\}_2]$, which was prepared according to the reference.[1,2]

Table S1

Table S1. Crystal data and structure refinement for compound **2**.

Compound	**2**
CCDC No.	1961099
Empirical formula	$C_{176}H_{170}N_{12}O_{23}P_2V_6Zn_2$
Formula Weight	3319.55
Crystal Size [mm^3]	0.300×0.300×0.040
T [K]	293(2)
λ [Å]	1.54184
Crystal system	monoclinic
Space group	$P2_1/c$
a [Å]	23.8905(7)
b [Å]	15.7761(3)
c [Å]	28.8721(8)
α [°]	90
β [°]	104.740(3)
γ [°]	90
V [Å^3]	10523.7(5)
Z	2
ρ_{calcd} [g cm^{-3}]	1.048
μ [mm^{-1}]	2.971
F (000)	3444
θ range [°]	3.532 to 67.509
Reflections collected	40650
Independent reflections	18924[R_{int}= 0.0697, R_{sigma}= 0.1306]
$R_1[I > 2\sigma(I)]$[a]	R_1= 0.0958, wR_2= 0.2353
wR_2 (all data)[b]	R_1= 0.1413, wR_2= 0.2680
GOF on F^2	1.013

[a] $R_1 = \Sigma||F_o| - |F_c||/\Sigma|F_c|$. [b] $wR_2 = [\Sigma w(F_o^2 - F_c^2)^2/\Sigma w(F_o^2)^2]^{1/2}$

Table S2

Table S2. Hydrogen bonding interactions and C-H···π interactions of compound **2**.

H-Bonds	D-A [Å]	A…H [Å]	D-H…A [◦]	Labels
C74-H74…O9	3.17	2.33	151.24	d2
C86-H86…O10	3.40	2.69	133.88	d3
C-H···π interactions	C-center [Å]	Center…H [Å]	C-H…Center [◦]	Labels
C80-H80···PlaneC32-C37	3.62	2.81	147.03	d1
C41-H41b···PlaneC32-C37	4.13	3.19	164.19	d4
C60-H60b···PlaneC42-C47	4.05	3.37	130.07	d5

1. Synthesis of Porphyrin Organic Building Blocks

The general synthetic process of the porphyrins is shown in the scheme below.

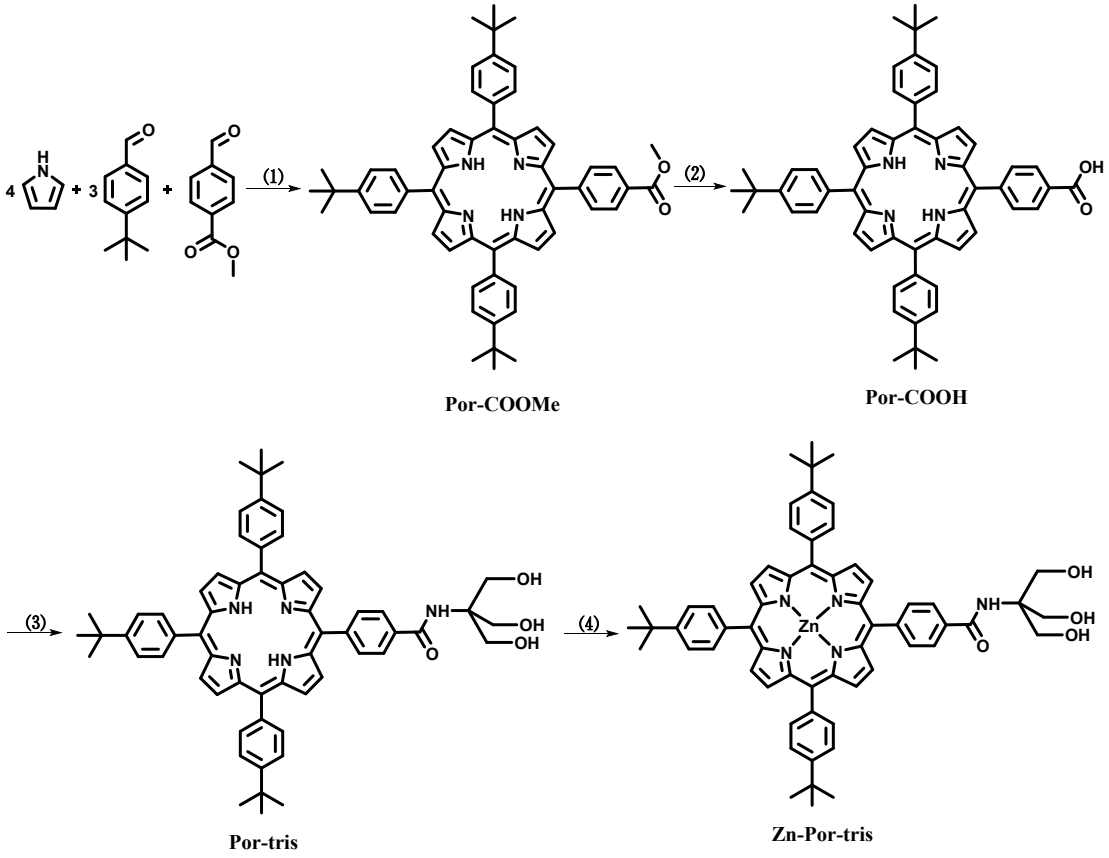

Scheme S1. Synthetic Scheme of the Porphyrin Building Blocks. (1) $BF_3 \cdot OEt_2$, DDQ, CH_2Cl_2, RT; (2) CH_3CH_2OH, NaOH, reflux; (3) Tris, DMAC, EEDQ, 60℃; (4) $Zn(OAc)_2 \cdot 2H_2O$, $CHCl_3/CH_3OH$, reflux.

Synthesis of Por-COOMe and Por-COOH. Por-COOMe and Por-COOH are synthesized according to the previously literature.[3] ^{1}H NMR of Por-COOMe ($CDCl_3$, 400 MHz, RT) [δ(ppm)]: -2.76 (s, 2H), 1.61 (s, 27H), 4.12 (s, 3H), 7.77(d, 2H), 8.14 (d, 6H), 8.32 (d, 2H), 8.44 (d, 2H), 8.77 (d, 2H), 8.88 (m, 6H). ESI-MS ($C_{58}H_{56}N_4O_2$): $[M+H]^+$, 841.4; ^{1}H NMR of Por-COOH ($CDCl_3$, 400 MHz, RT) [δ(ppm)]: -2.76 (s, 2H), 1.61 (s, 27H), 7.77(d, 6H), 8.15 (d, 6H), 8.35 (d, 2H), 8.50 (d, 2H), 8.77 (d, 2H), 8.88 (m, 6H); ESI-MS($C_{57}H_{54}N_4O_2$): $[M+H]^+$, 827.4.

Synthesis of Por-tris. Mixture of Por-COOH (1 g, 1.2 mmol), Tris (1.2 eq,180 mg), EEDQ (1.2 eq, 360 mg), DMAC (24 mL) in a 50 mL round bottle was stirred for 20h at 60 ℃. After the reaction temperature was cooled down to the room temperature, the mixture was dropped into 500mL deionized water and the resulted purple precipitate was collected by centrifugation and dried. The crude product was dissolved in a small amount $CHCl_3$ and purified with column chromatography with CH_3OH/dichloromethane = 4% (v:v) as eluent. The pure purple product of Por-tris was obtained by crystallization in pentane (m=668 mg, yield=60%).

^1H NMR of Por-tris (d_6-DMSO, 400 MHz, RT) [δ(ppm)]: -2.92 (s, pyrrole NH, 2H), 1.58 (s, CH_3, 27H), 3.85(d, CH_2, 6H), 4.90 (s, OH, 3H), 7.70 (s, NH, 1H), 7.85 (d, Ar-H, 6H), 8.16 (d, Ar-H, 6H), 8.30 (q, Ar-H, 4H), 8.85 (m, pyrrole-H, 8H); ESI-MS($C_{61}H_{63}N_5O_4$): [M-1], 928.4. UV-vis(DMF)[λ_{max}/nm]: 418 (Soret band), 515 550, 593, 648(Q bands); FT-IR(diamond)[cm^{-1}]: 3309(w), 2956(m), 2900(w), 2866(w), 1656(w), 1649(w), 1643(m), 1608(w), 1535(w), 1500(w), 1473(m), 1396(w), 1348(w), 1267(w), 1222(w), 1193(w), 1109(m), 1024(m), 1010(w), 993(w), 981(w), 966(s), 798(s), 733(s), 710(w).

2. ^{1}H-NMR

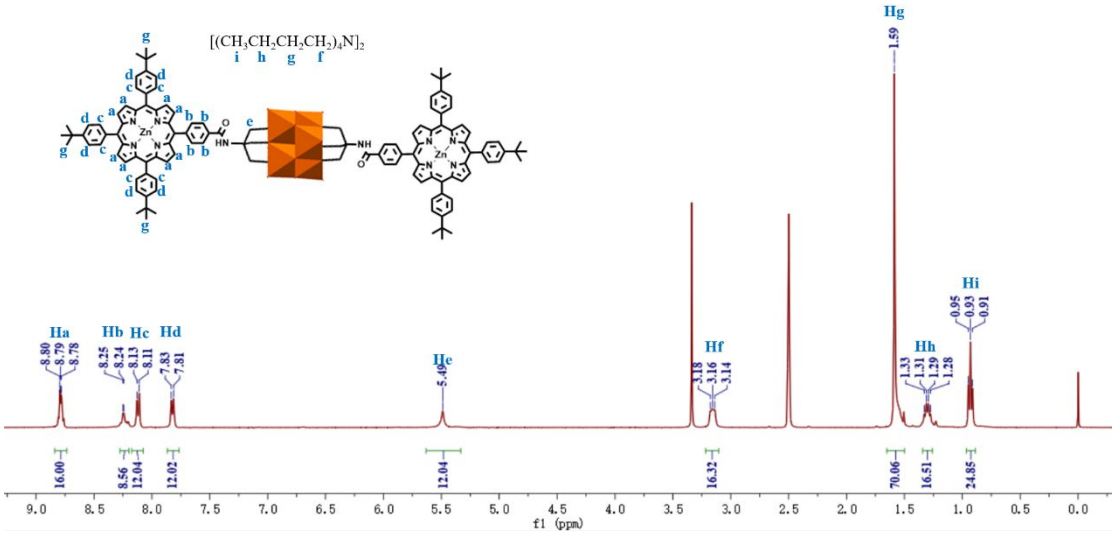

Figure S1. ^{1}H-NMR spectrum of Compound **1**.

^{1}H-NMR signals assignment for compound **1**: The peaks from downfield to high-field are labeled **Ha** to **Hi**. The multiple signal at 8.80ppm (Ha) is assigned to the peripheral H of the four pyrrole rings. The multiplet signal at 8.25ppm (Hb) is the H of benzene ring which is connected with the amide group. The double peaks at 8.11-8.13ppm (Hc) and 7.81-7.83ppm (Hd) are the inner H and outer H of benzene ring, respectively. The single peak at 5.49ppm (He) is the methylene H. The triplet at 3.14-3.18ppm (Hf) is the methylene H in tetrabutyl ammonium (TBA). The single peak at 1.59ppm (Hg) is the combination of peripheral tertiary butyl and partly methylene of TBA. The multiple peak at 1.28-1.33ppm (Hh) is the methylene H in TBA. The triplet signal at 0.91-0.95ppm (Hi) is the methyl H in TBA.

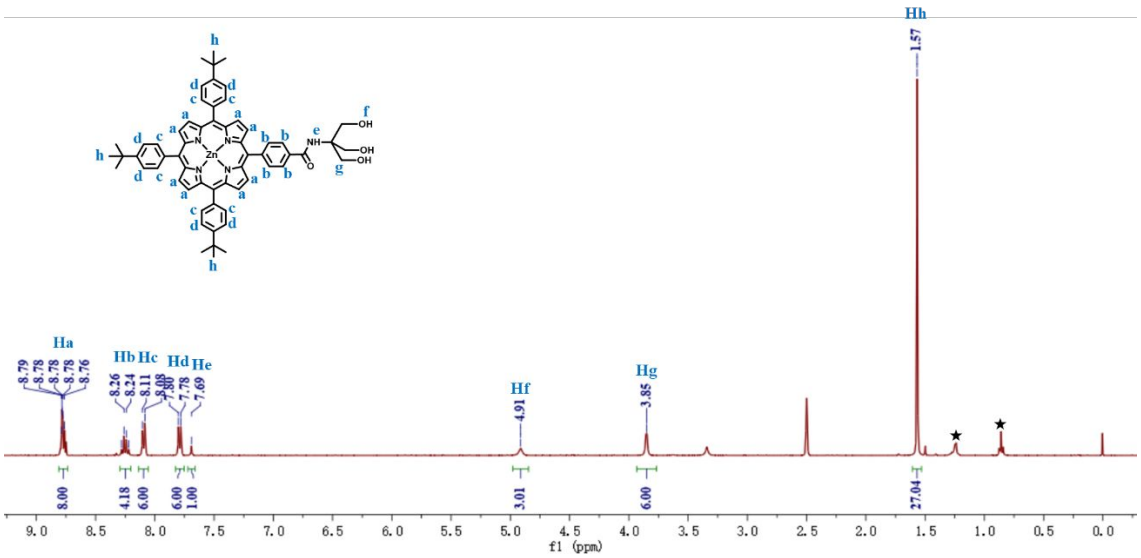

Figure S2. [1]H-NMR spectrum of **Zn-Por-tris**.

[1]H-NMR signal assignments for Zn-Por-tris: The peaks from downfield to high-field are labeled **Ha** to **Hh**. The multiple signal at ~8.78ppm (Ha) is assigned to the peripheral H of the four pyrrole rings. The quadruple signal at 8.22-8.28ppm (Hb) is the H of benzene ring which is connected with the amide group. The double peaks at 8.08-8.11ppm (Hc) and 7.78-7.80ppm (Hd) are the inner H and outer H of benzene ring, respectively. The minor single peak at 7.70ppm (He) is the NH of the amide group. The signal at 4.90ppm (Hf) is OH. The peak at 3.85ppm (Hg) is the methylene H. The single peak at 1.57ppm (Hh) is the H of peripheral tertiary butyl. The signal at 0.86 and 1.25ppm labeled by ★ is the residue of n-hexane used in the recrystallization process.

3. ESI-MS analysis

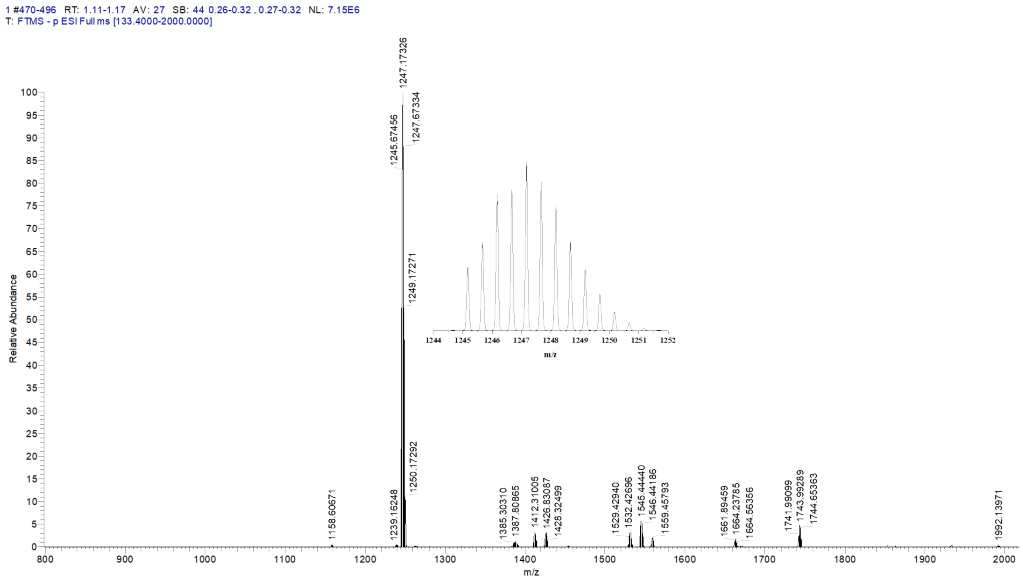

Figure S3. ESI-MS spectrum of compound **1** using the crystal precipitated from the liquid-diffusion solution of DMF/ diethyl ether. The inset is the enlarged part of m/z=1247.17.

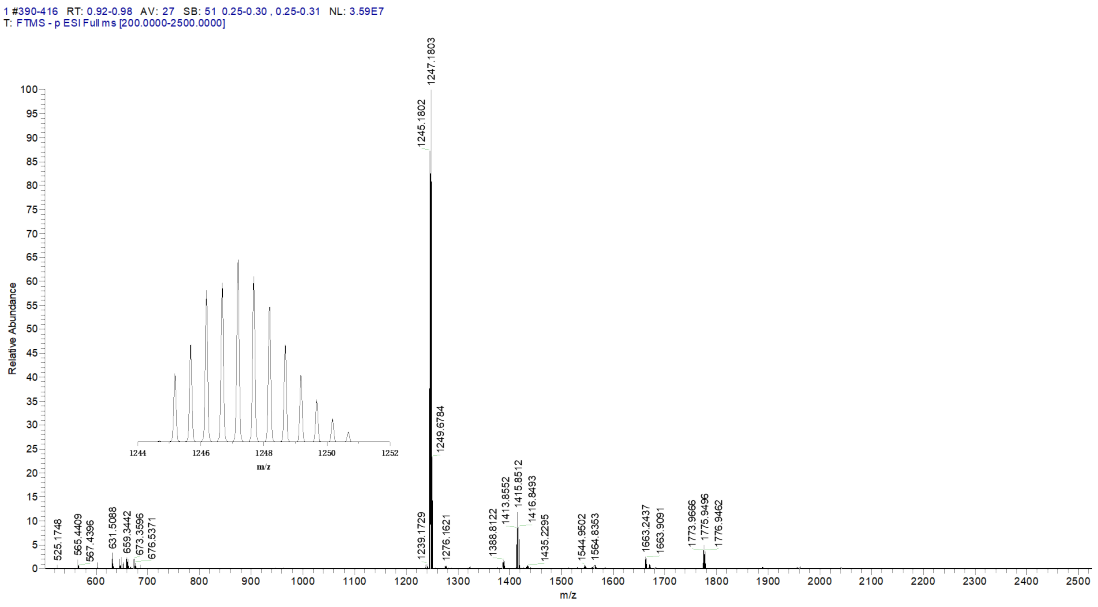

Figure S4. ESI-MS spectrum of compound **2** using the crystal precipitated from the solution of DMF. The inset is the enlarged part of m/z=1247.18.

4. FT-IR

Both characteristic peaks of Lindqvist structure and porphyrin organic ligands are existed in compounds **1**. The sharp and strong bands at 950 cm^{-1}, 717 cm^{-1} are corresponding to the vibration of V=O and V-O-V in the typical hexavanadate structure, respectively. The bands at 1051 cm^{-1} can be assigned to the vibration of C-O (Figure S5). Since the electron-withdrawing effect of the POMs, the hybrid exhibits high-wavenumber shift compared to the υ(C-O) of triol-porphyrin ligand **Zn-Por-tris** (Figure S6), which appeared at 1030 cm^{-1}. Additionally, the sharp and strong peak at around 796 cm^{-1} represented for the para-disubstituted benzene, verifying the existence of porphyrin ligands in both compounds **1**. Moreover, there is also a strong band at 998 cm^{-1}, which can be attributed to the vibration of Zn-N.

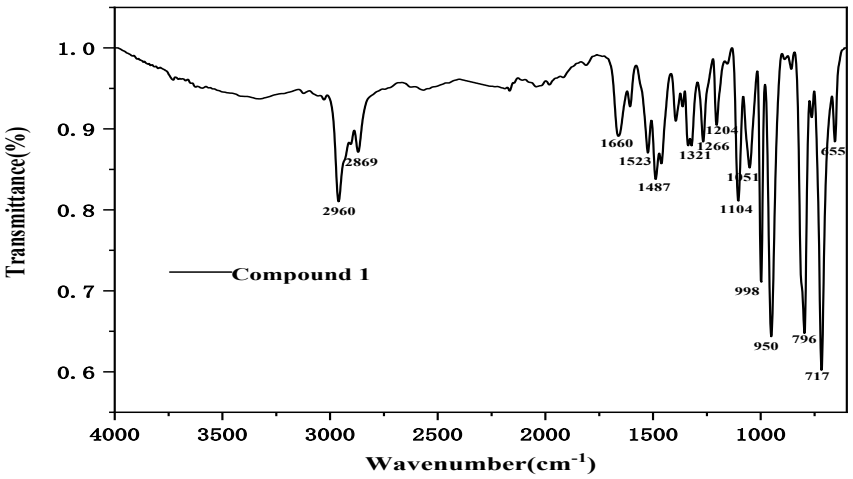

Figure S5. FT-IR spectrum of compound **1**.

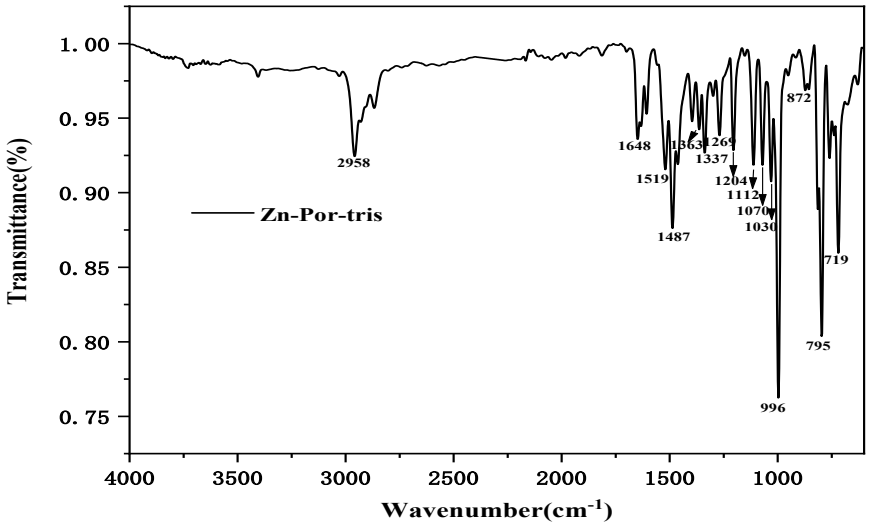

Figure S6. FT-IR spectrum of **Zn-Por-tris**.

5. UV-Vis absorption and emission spectra

The **Zn-Por-tris** and compound **1** present similar Soret bands at about 426 nm, meanwhile, their doubled Q bands are both located at 557 and 600 nm. The absorption positions of compound **1** are almost the same as the porphyrin precursor. This result indicates that there are no electron interactions between POMs and the porphyrin ligands at the ground state.

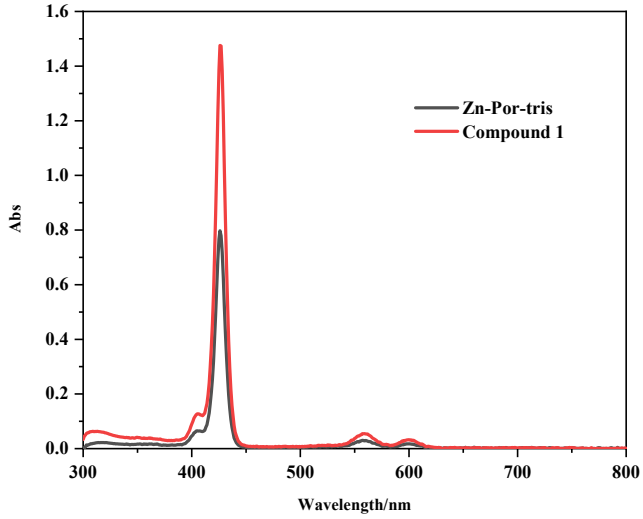

Figure S7. UV-vis absorption spectra of **Zn-por-tris** and compound **1**.

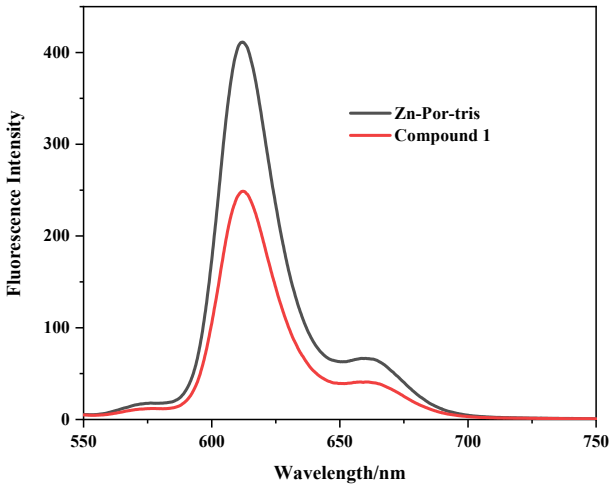

Figure S8. Emission spectra of **Zn-Por-tris** and compound **1** at the excitation wavelength of 429 nm.

6. Photocatalytic activities

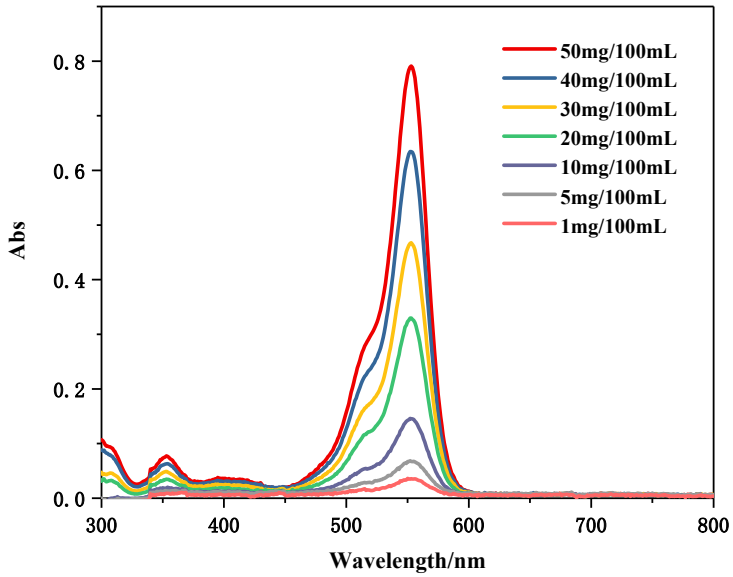

Figure S9. The standard curve of RhB in the aqueous solution.

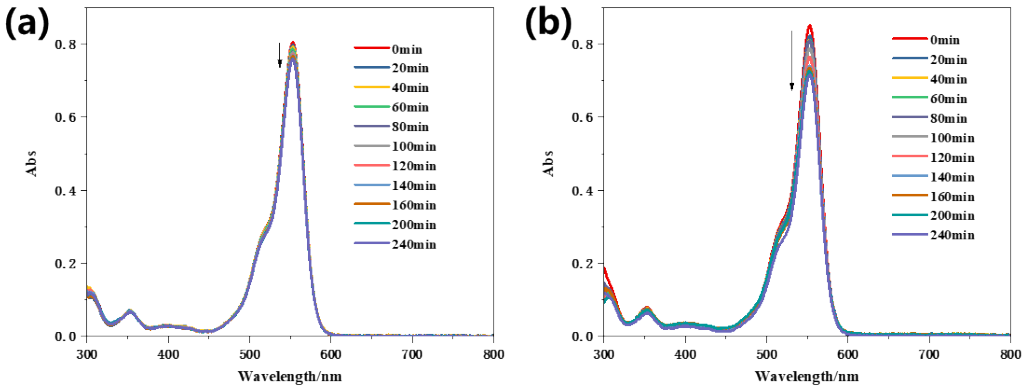

Figure S10. The UV-Vis spectra changes without catalyst a) dark, b) under visible-light.

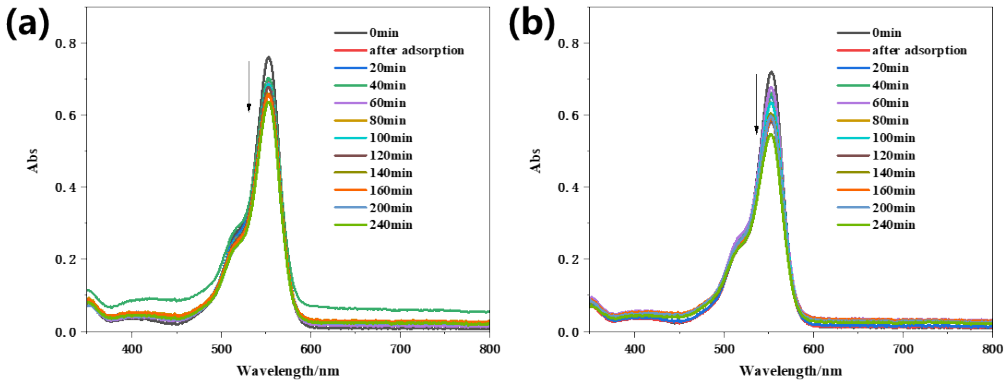

Figure S11. The UV-Vis spectra changes of Zn-Por-tris a) dark; b) under visible-light.

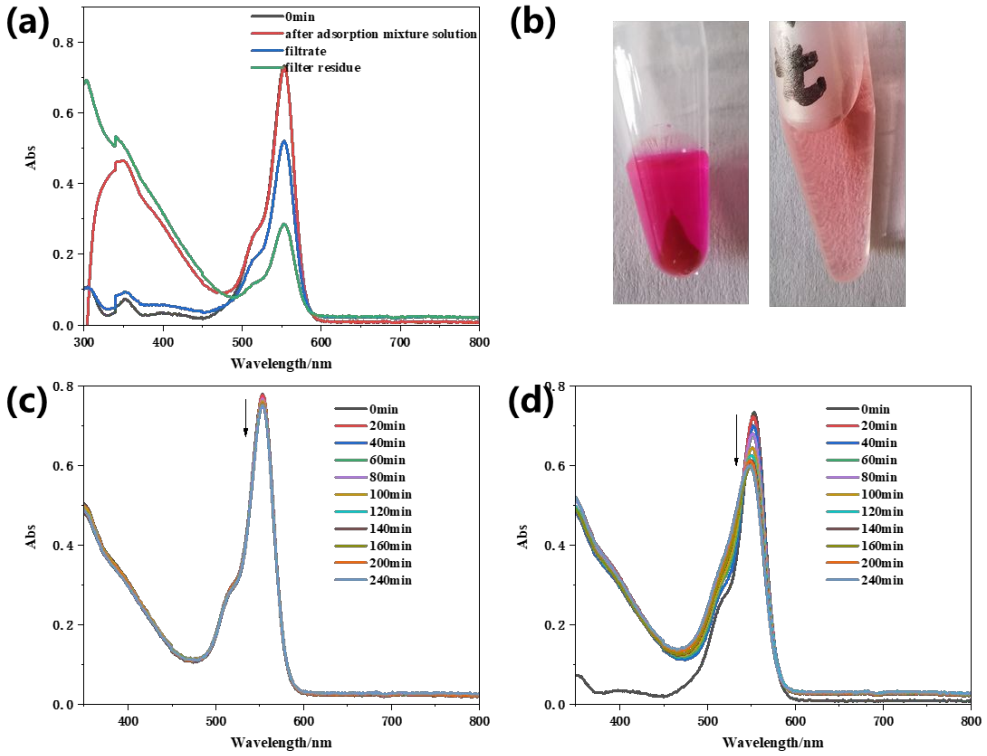

Figure S12. The UV-vis spectra changes of V10 a) with different solution; b) dark; c) under visible-light.

Using V10 as the catalyst, some red precipitates was generated in the solution after 1.5h dark adsorption (see Figure S12b left). After centrifugation, the UV-vis absorption of filtrate was showed in Figure S12a (the blue curve), exhibiting greatly decreased

absorption. However, the filter residue could also be dissolved in water (see Figure S12b right), the UV-vis absorption was given as the green curve in Figure S12a. The green curve not only reveals the characteristic absorption of RhB at 553nm, but also reveals the characteristic absorption of V10 at 300-450nm, which means that the red precipitate contains both V10 and RhB. This may be ascribed to some counter-ion exchange happened between RhB and V10, since RhB is a cationic dye, V10 with tetrabutylammonium counter-ion also has some solubility in water. So, exclude the effect of ion exchange, UV-vis was monitored directly from the reaction solution.

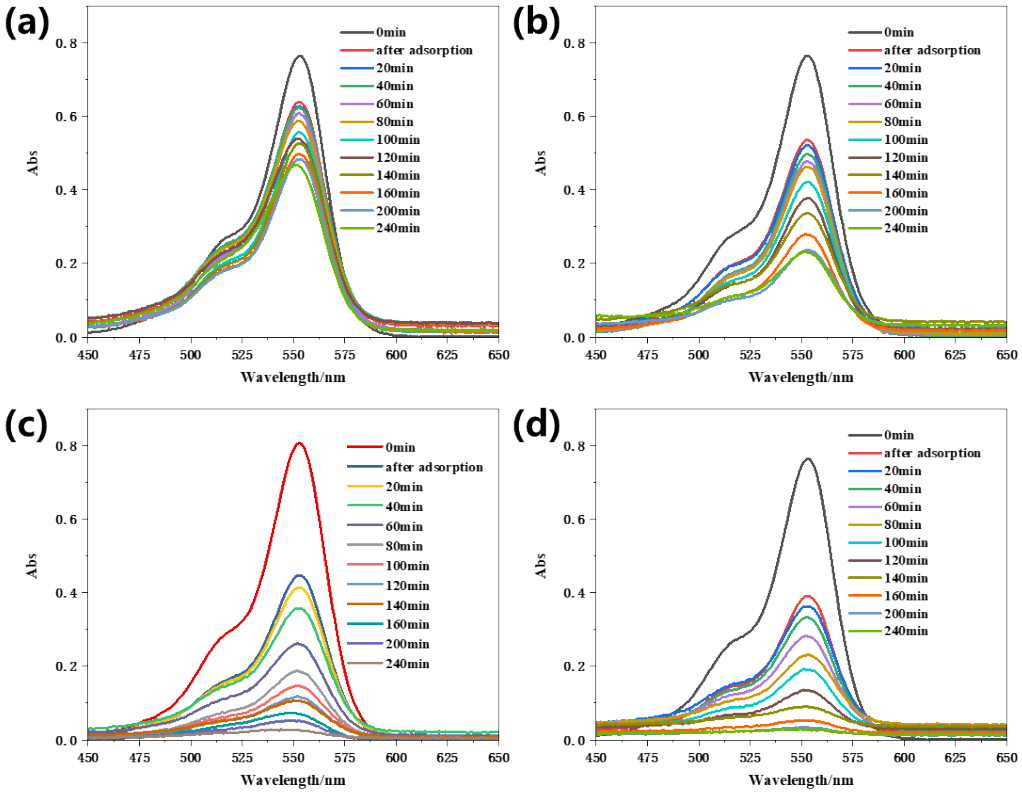

Figure S13. The UV-vis spectra changes of catalyst 1 under visible-light a) 3 mg; b) 6 mg; c) 9 mg; d) 12 mg

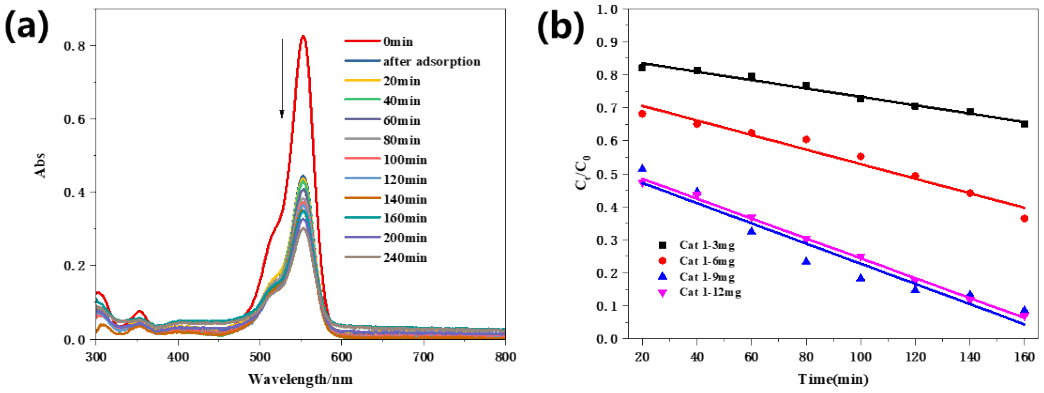

Figure S14. The UV-vis spectra changes of catalyst **1** a) under dark; b) linear changes of different catalytic amount of **1**.

7. FT-IR spectra before and after photocatalysis

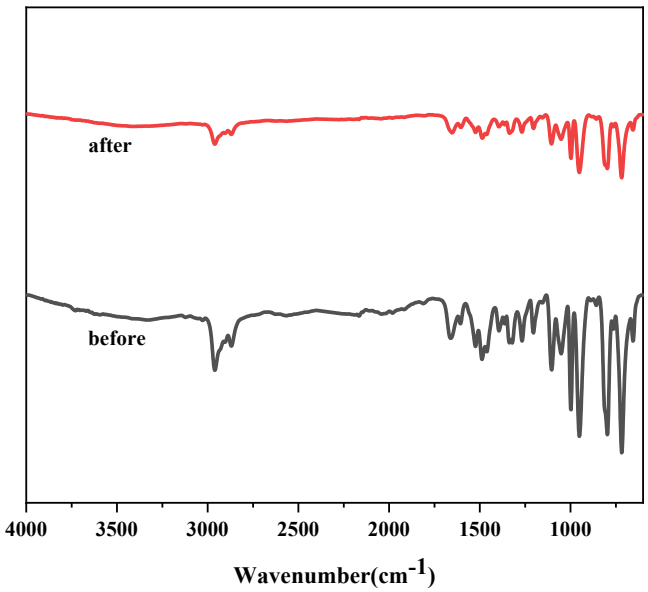

Figure S15. The FT-IR spectra of catalyst **1** before and after the catalytic process.

8. Energy bandgap calculation and CV results

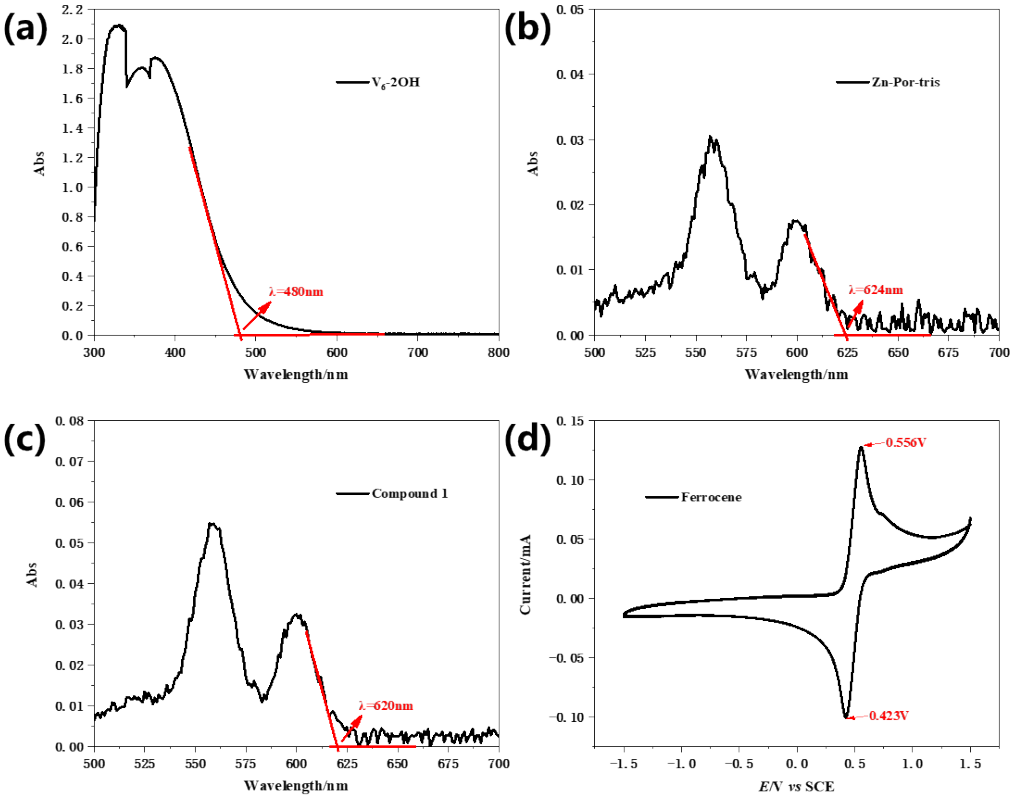

Figure S16. (a-c) UV-vis absorption edge of V6, Zn-Por-tris, compound **1** respectively. (d) cyclic voltammetry curve of ferrocene standard. V6 represents $(Bu_4N)_2[V_6O_{13}\{(OCH_2)_3CCH_2OH\}_2]$.[1]

Table S3

Table S3. Energy bandgap and HOMO-LUMO levels

Compound	λ_{max}(nm)[a)]	Eg(eV)[b)]	Ered(V vs SCE)[c)]	E_{LUMO}(eV)[d)]	E_{HOMO}(eV)[e)]
Zn-Por-tris	624	1.99	-1.22	-3.09	-5.08
Compound 1	620	2.0	-1.15	-3.16	-5.16
V_6	480	2.58	-0.47	-3.84	-6.42

a). Estimated from the absorption edge of UV-vis; b). estimated from the equation of E_g=1240/λ (λ is absorption edge); c). measured from the onset reduction potential of CV; d). estimated from equation E_{LUMO}(eV)=-[E_{red}-E_{FOC}+4.8]eV, E_{FOC}=(E_{ox}+E_{red})/2 of ferrocene used as standard. e). E_{HOMO}(eV)=E_{LUMO}-E_g

References

1. Chen, Q.; Goshorn, D. P.; Scholes, C. P.; Tan, X. L.; Zubieta, J. Coordination compounds of polyoxovanadates with a hexametalate core. Chemical and structural characterization of $[V^{V}_{6}O_{13}[(OCH_2)_3CR]_2]^{2-}$, $[V^{V}_{6}O_{11}(OH)_2[(OCH_2)_3CR]_2]$, $[V^{IV}_{4}VV_2O_9(OH)_4[(OCH_2)_3CR]_2]^{2-}$, and $[V^{IV}_{6}O_7(OH)_6\{(OCH_2)_3CR\}_2]^{2-}$. *J. Am. Chem. Soc.* **1992,** *114*, 4667-4681.
2. Wu, P.; Chen, J.; Yin, P.; Xiao, Z.; Zhang, J.; Bayaguud, A.; Wei, Y. Solvent-induced supramolecular chirality switching of bis-(trisalkoxy)-hexavanadates. *Polyhedron* **2013,** *52*, 1344-1348.
3. Wessendorf, F.; Gnichwitz, J.-F.; Sarova, G. H.; Hager, K.; Hartnagel, U.; Guldi, D. M.; Hirsch, A. Implementation of a Hamiliton-Receptor-Based Hydrogen-Bonding Motif toward a New Electron Donor−Acceptor Prototype: Electron versus Energy Transfer. *J. Am. Chem. Soc.* **2007,** *129*, 16057-16071.